ENERGY-PRESERVING TIME-VARYING SCHROEDER ALLPASS FILTERS

Kurt James Werner

iZotope, Inc., Cambridge, MA
kwerner@izotope.com

ABSTRACT

In artificial reverb algorithms, gains are commonly varied over time to break up temporal patterns, improving quality. We propose a family of novel Schroeder-style allpass filters that are energy-preserving under arbitrary, continuous changes of their gains over time. All of them are canonic in delays, and some are also canonic in multiplies. This yields several structures that are novel even in the time-invariant case. Special cases for cascading and nesting these structures with a reduced number of multipliers are shown as well. The proposed structures should be useful in artificial reverb applications and other time-varying audio effects based on allpass filters, especially where allpass filters are embedded in feedback loops and stability may be an issue.

1. INTRODUCTION

Manfred Schroeder's work on artificial reverb in the 1960s [1, 2] introduced the "Schroeder" allpass filter (sometimes called the "comb allpass"): a high-order, low-complexity allpass filter characterized by the length of its single delay line and a single gain coefficient. These are ubiquitous today. Schroeder allpass filters are also commonly seen in "nested form," following or preceding the delay line(s) inside of comb filters [3, 4], Feedback Delay Networks [5–8], or even another Schroeder allpass [2, 9–13]. Recent work by Schlecht generalizes the Schroeder design, allowing the allpass gain to be replaced by any stable filter whose magnitude response is bounded by unity [14]. Time-varying 1st-order allpass filters (which can be considered a specific case of Schroeder allpasses with a delay line length of 1) have also been explored widely in digital audio effect and synthesizer design [8, 15–23].

Although reverb algorithms are almost always designed from a linear time-invariant (LTI) prototype, it is common to vary gains over time to break up resonances [3, 6, 9, 24–27]. It is essential in varying these gains that the structure's stability be preserved, which can be accomplished by preserving the signal energy during variation. Unfortunately, the Schroeder allpass filter has been shown not to preserve energy as its coefficient is changed [6].

In this paper, we address this issue by introducing a novel family of Schroeder-style allpass filters that are energy-preserving during arbitrary and continuous change of their gain coefficient.

The rest of this paper is structured as follows. §2 reviews Schroeder and 1st-order energy-preserving allpass filters. §3 proposes a family of novel, energy-preserving, time-varying Schroeder allpass filters. §4 presents strategies for reducing the number of multiplies in structures containing numerous proposed filters. §5 shows the proposed filters in action. §6 concludes.

2. PREVIOUS WORK

In this section we review the foundations of the proposed filter structures in this paper: Schroeder-style allpass filters (§2.1), a definition for the allpass property in the time-varying case (§2.2), and Bilbao's energy-preserving 1st order allpass filter (§2.3).

2.1. Classic LTI Schroeder allpass filters

Mth-order Schroeder allpass filter have the transfer function

$$H_M(z) = \frac{Y(z)}{X(z)} = \frac{\overline{g} + z^{-M}}{1 + gz^{-M}} \,. \tag{1}$$

Taking $M = 1$ gives the case of a 1st-order allpass filter. Evaluating the transfer function at $z = e^{-j\omega}$

$$H_M(e^{-j\omega}) = \frac{\overline{g} + \mathrm{e}^{-j\omega M}}{1 + g\mathrm{e}^{-j\omega M}} = \frac{\mathrm{e}^{-j\omega M}\left(1 + \overline{g}\mathrm{e}^{+j\omega M}\right)}{1 + g\mathrm{e}^{-j\omega M}} \tag{2}$$

and noting that $\left|\mathrm{e}^{-j\omega M}\right| = 1$ and $\left|1 + \overline{g}\mathrm{e}^{+j\omega M}\right| = \left|1 + g\mathrm{e}^{-j\omega M}\right|$ verifies that Schroeder allpass filters have unit magnitude response:

$$|H_M(z)| = 1 \longrightarrow |X(z)| = |Y(z)| \;, \forall\omega \,. \tag{3}$$

Specifically, in this paper as with most audio applications, we are concerned with the real-valued version with $\overline{g} = g \in \mathbb{R}$.

2.2. Energy-Preserving, Time-Varying Allpass

The z-transform cannot be used to characterize time-varying filters. This makes the standard frequency-domain definition of the allpass property (3) impossible to apply. Therefore, we must instead consider a property in the time-domain.

According to the discrete-time Parseval's theorem

$$\sum_{n=-\infty}^{\infty} |x_n|^2 = \frac{1}{2\pi}\int_{-\pi}^{\pi} |X(\omega)|^2 \,\mathrm{d}\omega \,,$$

(3) implies, in the time-domain [8, p. 74] [15]:

$$||y_\cdot|| = ||x_\cdot|| \,, \; \forall x_n \tag{4}$$

where $||f_\cdot||$ is the L2-norm (energy) of f_n:

$$||f_\cdot|| = \left(\sum_{n=-\infty}^{\infty} f_n^2\right)^{1/2} . \tag{5}$$

Since the filter output's energy is equal to the filter input's energy, we say that it is *energy-preserving* (or "lossless"). The property (4) can be considered for time-varying systems as well. An energy-preserving time-varying allpass filter should satisfy (4) for a time-varying gain, and (3)–(4) for a non-time-varying gain (LTI case).

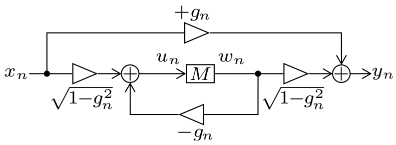

Figure 1: *Bilbao's energy-preserving allpass filter ($M = 1$) and the normalized (type V) proposed structure ($M \geq 1$).*

2.3. Bilbao's time-varying allpass

In [15], Bilbao proposed several special allpass filters that fulfill property (4). Here we review one which consists of two blocks.

First: A 1-sample delay[1], of signal u_n

$$w_n = u_{n-1}\,. \tag{6}$$

Since it is just a shift of the time index, it is simple to verify

$$||w_\cdot|| = ||u_\cdot||\,, \tag{7}$$

so a 1-sample delay is norm-preserving.

Second: An orthogonal matrix multiplication[2] of the vector $\begin{bmatrix} x_n & w_n \end{bmatrix}^\top$ (input x_n and delay-line output w_n) by matrix $\mathbf{\Pi}_n$

$$\begin{bmatrix} y_n \\ u_n \end{bmatrix} = \begin{bmatrix} g_n & \sqrt{1-g_n^2} \\ \sqrt{1-g_n^2} & -g_n \end{bmatrix} \begin{bmatrix} x_n \\ w_n \end{bmatrix}\,, \tag{8}$$

producing vector $\begin{bmatrix} y_n & u_n \end{bmatrix}^\top$ (filter output y_n and delay-line input u_n). This verifies

$$||x_\cdot|| + ||w_\cdot|| = ||y_\cdot|| + ||u_\cdot|| \tag{9}$$

by the definition of $\mathbf{\Pi}_n$'s orthogonality. The matrix's orthogonality can easily be seen since $\mathbf{\Pi}_n^\top \mathbf{\Pi}_n = \mathbf{I}$, where $\mathbf{I}$ is the 2×2 identity matrix.[3] Fig. 1 shows a block diagram of this structure.

By subtracting (7) from (9), we recover (4), showing that the structure is energy-preserving. In the special case of a fixed coefficient $g_n = g\,\forall n$, this filter has a standard allpass transfer function

$$H_{\text{Bilbao}}(z) = \frac{Y(z)}{X(z)} = \frac{g + z^{-1}}{1 + gz^{-1}}\,. \tag{10}$$

3. PROPOSED EXTENSIONS

In this section, we will propose a number of extensions to Bilbao's design, which yield a family of new energy-preserving allpass filter structures. These new structures exploit two main insights:

1. Energy preservation remains valid if the unit delay is replaced by *any* L2-norm-preserving block,
2. Besides four scalar multiplies, there are many ways to implement the orthogonal matrix multiply $\mathbf{\Pi}_n$.

[1] Bilbao [15] uses the Wave Digital Filter (WDF) formalism [28, 29] in his article, where (6) can be interpreted as a WDF model of a capacitor.

[2] In WDF terms, (8) is a 2-port power-wave parallel junction [15,28,29].

[3] Considering the delay as a particular case of a time-varying reactance with the formalism used in [47], this is a power-wave simulation using Fettweis' time-varying reactance model. We might wonder if the flexibility in time-varying reactance modeling provided by [47] and wave variable choice provided by [29] might produce alternate structures similar to Bilbao's design. However, they appear not to.

The first insight allows us to create more complex energy-preserving allpass filters. Specifically, we focus on building high-order, low-complexity (few multipliers) Schroeder-style allpass filters commonly used in audio processing, especially artificial reverb and more complex *nested* allpass filters [9–13], both of which enjoy the same energy-preservation property.

The second insight allows us to propose a large class of structures for implementing a given time-varying allpass filter design, including some that are canonic in both delays and multipliers. These structures all have the same time-varying behavior, but different implementation tradeoffs. In addition to the novelty of ensuring energy preservation in these structures, many of these structures have not been seen in the LTI Schroeder allpass context or even the LTI 1st-order allpass context.

To present these findings, we will first discuss the algorithm's building blocks (§3.1), give a recipe for assembling structures from those blocks (§3.2), and finally comment on these structures (§3.3).

3.1. Building blocks

On top of generalizing Bilbao's design in these ways, we can also generalize how the multiplication by orthogonal matrix $\mathbf{\Pi}_n$ is implemented. That is, we will use different arrangements of adds, multiplies, and sign flips to implement that matrix multiplication.

Fig. 2 shows the building blocks of the proposed method:

1. A direct implementation of the multiplies in a two-port[4] $\mathbf{\Lambda}_n$ is shown in Fig. 2a. Nine specific ladder/lattice two-ports are shown in Figs. 2b–2j. These two-ports are parameterized by a time-varying gain $-1 < g_n < +1$. Schroeder's original designs allow the gain g_n to go all the way to the extremal values ($-1 \leq g_n \leq +1$). However, that leads to marginally stable filters even in the LTI case, and here leads to multiplier values of $\pm\infty$, so we enforce $g_n \neq \pm 1$.
2. A "transformer" pair of reciprocal multiplies with two-port matrix $\mathbf{\Xi}_n = \left[\begin{smallmatrix} 0 & 1/\xi_n \\ \xi_n & 0 \end{smallmatrix}\right]$ is shown in Fig. 2k; the transformers multipliers are shaded throughout just to make them easier to identify in the structures.
3. Finally, the length-M delay line is shown in Fig. 2l.

The nine two-ports come from the classic ladder/lattice synthesis literature [30–32] and simple generalizations. The original is the "Kelly-Lochbaum" 4-multiply [33] (Fig. 2c); we also consider its transpose (Fig. 2d). The 3-multiply (Fig. 2e) was introduced in ladder filter synthesis [31]; we also consider its transpose (Fig. 2f). Simpler still are the 2-multiply "lattice" two-port [31] (Fig. 2g) and its transpose [34] (Fig. 2h) which implement the same matrix multiplication as the 3-multiply and its transpose. Next is the 1-multiply (Fig. 2i) and its transpose [31] (Fig. 2j), which each involve a sign flip and implement the same matrix multiplication as the 4-multiply and its transpose.[5] Finally, we have the power-normalized two-port [32] (Fig. 2b).

All nine two-ports can be described with five different types of $\mathbf{\Lambda}_n$ (Fig. 2a). Each type except the power-normalized has two implementations. The multipliers $\lambda_{11,n}$, $\lambda_{12,n}$, $\lambda_{21,n}$, and $\lambda_{22,n}$ for each type are given in Tab. 1. Notice that $\lambda_{11,n} = +g_n$ and $\lambda_{22,n} = -g_n$ for all types. The transformer $\mathbf{\Xi}_n$ needed to create an orthogonal matrix $\mathbf{\Pi}_n$ is shown as well. Notice that for transposed structures, $\lambda_{12,n}$ and $\lambda_{21,n}$ swap places, and ξ_n is inverted.

[4] "Two-ports" are blocks with two pairs of inputs and outputs.

[5] In the literature these have opposing "sign parameters." We will call them transposes for consistency with the other types.

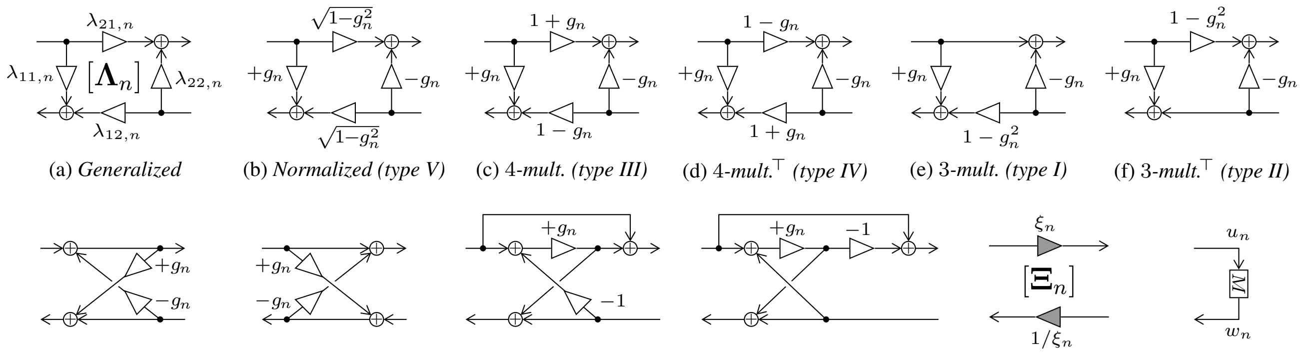

(a) *Generalized* (b) *Normalized (type V)* (c) 4-*mult. (type III)* (d) 4-*mult.*$^\top$ *(type IV)* (e) 3-*mult. (type I)* (f) 3-*mult.*$^\top$ *(type II)*

(g) 2-*mult. (type I)* (h) 2-*mult.*$^\top$ *(type II)* (i) 1-*mult. (type III)* (j) 1-*mult.*$^\top$ *(type IV)* (k) *Transformer* (l) M *Delays.*

Figure 2: *Building blocks of the proposed algorithm, including ladder/lattice two-ports, transformer, and delay line.*

Table 1: *Two-port entries, corresponding transformer gains and inverses, and difference equation coefficients for unnormalized structures.*

		two-port $\mathbf{\Lambda}_n$ entries				transformer mult. & inverse		Un-corrected difference equation coefficients		
name	type	$\lambda_{11,n}$	$\lambda_{12,n}$	$\lambda_{21,n}$	$\lambda_{22,n}$	ξ_n	$1/\xi_n$	$b_{0,n}$	$b_{M,n}$	$a_{M,n}$
1- & 4-mult.	III	$+g_n$	$1-g_n$	$1+g_n$	$-g_n$	$\sqrt{\frac{1-g_n}{1+g_n}}$	$\sqrt{\frac{1+g_n}{1-g_n}}$	$+g_n$	$\frac{1-g_n}{1-g_{n-M}}$	$g_{n-M}\frac{1-g_n}{1-g_{n-M}}$
1- & 4-mult$^\top$	IV	$+g_n$	$1+g_n$	$1-g_n$	$-g_n$	$\sqrt{\frac{1+g_n}{1-g_n}}$	$\sqrt{\frac{1-g_n}{1+g_n}}$	$+g_n$	$\frac{1+g_n}{1+g_{n-M}}$	$g_{n-M}\frac{1+g_n}{1+g_{n-M}}$
2- & 3-mult.	I	$+g_n$	$1-g_n^2$	1	$-g_n$	$\sqrt{1-g_n^2}$	$1/\sqrt{1-g_n^2}$	$+g_n$	$\frac{1-g_n^2}{1-g_{n-M}^2}$	$g_{n-M}\frac{1-g_n^2}{1-g_{n-M}^2}$
2- & 3-mult.$^\top$	II	$+g_n$	1	$1-g_n^2$	$-g_n$	$1/\sqrt{1-g_n^2}$	$\sqrt{1-g_n^2}$	$+g_n$	1	g_{n-M}
Normalized	V	$+g_n$	$\sqrt{1-g_n^2}$	$\sqrt{1-g_n^2}$	$-g_n$	1	1	$+g_n$	$\sqrt{\frac{1-g_n^2}{1-g_{n-M}^2}}$	$g_{n-M}\sqrt{\frac{1-g_n^2}{1-g_{n-M}^2}}$

3.2. Recipe

Our strategy is to augment one of the two-ports ($\mathbf{\Lambda}_n$, Fig. 2b–2j) with an appropriate "transformer" pair of reciprocal multiplies ($\mathbf{\Xi}_n$, Fig. 2k). With the correct transformer coefficient ξ_n, this structure implements the same matrix multiplication as $\mathbf{\Pi}_n$. Finally, by terminating this two-port on a length-M delay line (Fig. 2l), we create an energy-preserving Schroeder allpass filter.

An orthogonal two-port $\mathbf{\Pi}_n$ is formed by cascading transformers and ladder/lattice two-ports in one of two orientations, as shown in Figs. 3a/3b. In general, two-ports do not commute—this is a special property of $\mathbf{\Xi}_n$. A proof given in Appendix A yields

$$\mathbf{\Pi}_n = \begin{bmatrix} \lambda_{11,n} & \lambda_{12,n}/\xi_n \\ \lambda_{21,n}\xi_n & \lambda_{22,n} \end{bmatrix}, \tag{11}$$

showing that, regardless of whether the transformer $\mathbf{\Xi}_n$ is inside or outside the ladder section $\mathbf{\Lambda}_n$, the result is a scattering matrix $\mathbf{\Pi}_n$ whose off-diagonal entries π_{12} and π_{21} are scaled down and up respectively by the transformer parameter ξ_n.

The resulting proposed filter structures are shown in Fig. 4. The power-normalized (type V) structure was already shown in Fig. 1 and has no distinction between transformer locations.

Each filter's time-varying difference equation has the form

$$y_n = b_{0,n}x_n + b_{M,n}x_{n-M} - a_{M,n}y_{n-M}\,. \tag{12}$$

Without the transformer, the 17 structures have 5 distinct difference equations, with coefficients given in the last three columns of Tab. 1. Once the normalizing transformer is added, all 17 have the same difference equation as the normalized (type V) case. We will not pursue this implementation further, nor any others involving g_{n-M}, since the need for access to previous multiplier values in computing $a_{M,n}$ and $b_{M,n}$ at least doubles the number of delay registers needed, compared to the traditional Schroeder allpass filters (from M to $2M$, or more if the coefficients themselves are delayed instead of g, or it is implemented in direct form). In contrast, all of the filter structures discussed in the rest of this paper are canonic in delays.

3.3. Discussion of proposed structures

None of the 16 structures shown in Fig. 4, nor the structure in Fig. 1 with $M \neq 1$, appear to have been reported before. The implementation costs of each filter structure—in terms of multiplies ($\times$), adds ($+$), sign inversions (inv.), and delay registers (T)—are shown in Tab. 2. The 2-multiplier and its transpose have the same cost as the normalized structure. The 3- and 4-mutliplier structures and their tranposes are more expensive. The 1-multiplier and its transpose have the fewest multiplies, although they require an extra add and a sign inversion compared to the other structures.

It's likely that the most interesting structures are those with the lowest cost (1-mult.$^{(\top)}$) and those resembling the common LTI embodiment (2-mult.$^{(\top)}$). It could be interesting to study the overflow, noise, and sensitivity of the different designs, but it is beyond the scope of the current study. Stilson's work on studying the different LTI allpass forms could be a guide [34].

By ignoring the reciprocal transformer multiplies, we obtain a family of 9 different LTI allpass filter structures (not 17, since the transformer "inside"/"outside" distinction does not apply in the

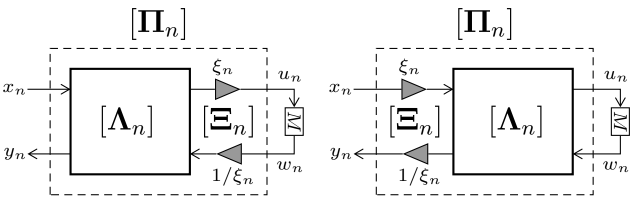

(a) *Transformer "inside."* (b) *Transformer "outside."*

Figure 3: *Two ways of forming an energy-preserving allpass filter from a two-port $\mathbf{\Lambda}_n$, transformer $\mathbf{\Xi}_n$, and length-M delay line.*

LTI case). Several of these were known in the literature already. The original Schroeder allpass was a 3-mult. version (Figs. 4i/j, w/o transformers). 2-mult. versions were used, e.g. in the "Sampson box" at CCRMA [40–42]; these are the versions (Figs. 4e–h, w/o transformers) most commonly encountered in the literature today [5, 9, 39]. It appears not to be very well-known, but Moorer also proposed a 1-multiply variant [43] (Figs. 4a/b, w/o transformers). Figs. 4c/d, k/l, and m/n appear to be novel.

Taking $M = 1$, certain 1st-order versions of these structures are known in the literature. Figs. 4a–d arise as a consequence of the "multiplier extraction" method [44]. Figs. 4e/f are known [8, 45]. Figs. 4g/h have been studied for their scaling properties [34].

Table 2: *Implementation costs of proposed filter structures.*

name	type	$\times$	$+$	inv.	T	total op.
1-mult. / 1-mult.$^\top$	III / IV	3	3	1	M	$M+7$
2-mult. / 2-mult.$^\top$	I / II	4	2	0	M	$M+6$
3-mult. / 3-mult.$^\top$	I / II	5	2	0	M	$M+7$
4-mult. / 4-mult.$^\top$	III / IV	6	2	0	M	$M+8$
normalized	V	4	2	0	M	$M+6$

Table 3: *Summary of cascaded allpasses with identical gains in reverbs. # AP denotes the number of allpasses in cascade and how many times that cascade appears in the structure. Gain(s) g lists the gains that are used in each cascade.*

author	name	# AP	gain(s) g
Manfred Schroeder [1]	"colorless"	2	0.7
Perry Cook [35]	PRCREV	2	0.7
John Chowning [8]	JCREV	3	0.7
John Chowning [8]	SATREV	3	0.7
Michael McNabb [36]	NREV	3	0.7
Jezar Wakefield [8]	Freeverb	4	0.5
Keith Barr [37, 38]	FV-1 demo	$2(\times 4)$	0.5
Jon Dattorro [39]	Plate	$2(\times 2)$	0.75, 0.625
William Gardner [9]	Large Room	$2(\times 2)$	0.3, 0.2

4. SPECIAL CASES WITH FEWER MULTIPLIES

We have derived energy-preserving versions of all known forms of the basic Schroeder allpass filter (and a few apparently unknown ones), which can be nested and cascaded while still retaining their energy preservation property. In this section, we will point out some special cases that form particularly efficient (in the sense of having few multiplies) filter structures: Cascades with identical and inverse gains (§4.1) and up to four distinct gains (§4.2), a "leapfrog" multiplier-sharing arrangement (§4.3), nestings (§4.4), and a strategy based on periodic modulation (§4.5). None of these proposed strategies put any restrictions on delay line lengths.

4.1. Identical- and inverse-multiplier cascades

For the filter structures with the transformer "outside," the transformer multiplies $\xi_{21,n} = \xi_n$ and $\xi_{12,n} = 1/\xi_n$ appear outside of any feedback loop as multiplications just after the input and just before the output, respectively. This means that when two of the proposed filters which have identical allpass gains g_n are cascaded, the reciprocal multiplies ξ_n and $1/\xi_n$ cancel out, saving two multiplies. This property holds true for any of the four unnormalized types: I–IV. It does nothing for the normalized case, however, since in that case $\xi_n = 1/\xi_n = 1$.

Although this is a special case, it is apparently an extremely common one. Most reverbs in the literature which employ Schroeder allpasses use identical gains for each one. A summary of the number of allpasses with identical gains in cascade for various reverbs is shown in Tab. 3. In Dattorro's plate reverb [39], each pair of "decay diffusers" has identical gains; however since they are not adjacent, this trick could not be used there.

For 2/3-multiply (type I) cases and their transposes (type II), this property also holds whenever $g_{i+1,n} = -g_{i,n}$. This type of design occurs, e.g., in another one of Schroeder's original reverbs [1], which has 5 allpasses in cascade with identical gains, up to a sign flip: $+0.7$, -0.7, $+0.7$, $+0.7$, $+0.7$.

In certain cases, we can also eliminate pairs of multiplies by alternating g's sign as well as alternating between 1-mult.$^{(\top)}$ implementations (type III/IV). If stage i is type III (resp. IV), switching to type IV (resp. III) in stage $i+1$ allows the pair of multiplies to be eliminated when $g_{i+1,n} = -g_{i,n}$. However, no such property holds for the 2/3-multiply (type I) or its transpose (type II).

Outside the reverb context, a cascade of many identical 1st-order allpasses can be used in string modeling [16]. This previously cost 4 multiplies per sample of maximum delay: $4N$ for N stages. The proposed method reduces this down to $N+2$, using 1-mult. or 1-mult.$^\top$, cutting $(3N-2)/4N \approx 75\%$ of the multiplies. The example in [16] has $N = 126$, so here the proposed method would yield significant savings: 376 multiplies per time step.

4.2. More general cascades

A more elaborate generalization of this property allows for non-identical gains. Recalling Tab. 1 and that the multiplier cancellation property comes from ξ_n being identical in two adjacent stages (satisfied automatically for identical topologies), notice that the multiplier cancellation can also be achieved in certain cases by choosing two different topologies and values for g.

Tab. 4 shows a set of functions, $f_{\text{type}_{i+1},\text{type}_i}()$, which choose a multiplier-saving gain $g_{i+1,n}$ for stage $i+1$ based on the gain $g_{i,n}$ of stage i. $f^{\pm}_{\text{III},\text{I}}$, $f^{\pm}_{\text{III},\text{II}}$, $f^{\pm}_{\text{IV},\text{I}}$, and $f^{\pm}_{\text{III},\text{II}}$ are multifunctions with positive and negative branches.

Several cases are degenerate in one way or another. First, there is no combination of $g_{i,n}$ and $g_{i+1,n}$ that allows transitioning to *or* from the power-normalized topology (type V). Second, $f_{\text{I},\text{II}}$ and $f_{\text{II},\text{I}}$ have domains and ranges of $\{0\}$—they are only valid for the

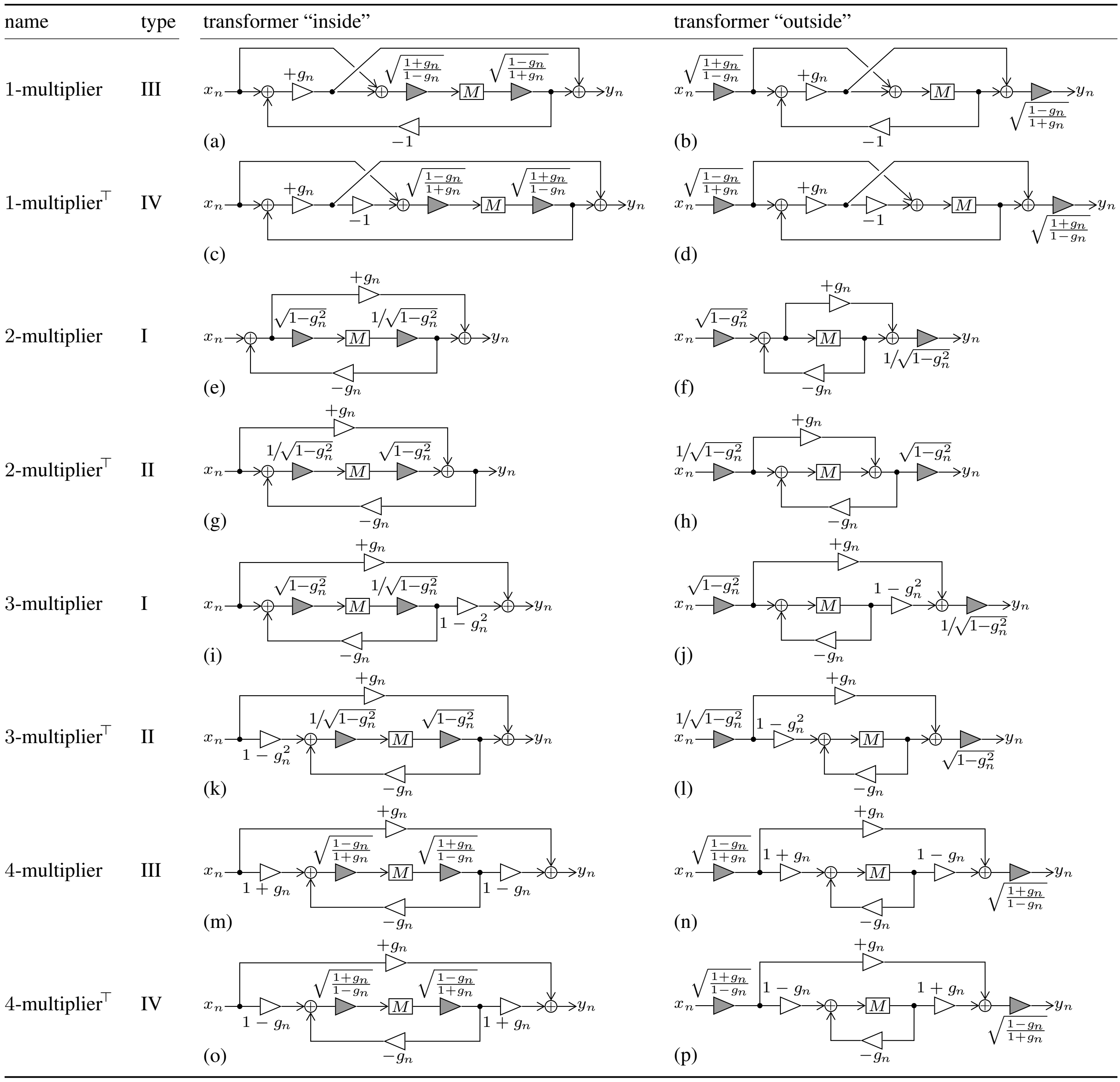

Figure 4: *Proposed allpass filter structures.*

useless case of $g_{i,n} = 0$, $\forall n$ (a trivial cascade of two pure delay lines). Also, not all gains g_i can be mapped to a compatible g_{i+1}, restraining the valid domain of the different $f()$

For example, starting with $g_{0,n} = 0.7$ can yield a cascade:

$$
\begin{aligned}
\text{type I:} &\quad g_{0,n} = +0.7 \\
\text{type III:} &\quad g_{1,n} \approx +0.3245 = f_{\text{I,III}}(g_{0,n}) \\
\text{type IV:} &\quad g_{2,n} \approx -0.3245 = f_{\text{III,IV}}(g_{1,n}) \\
\text{type I:} &\quad g_{3,n} = -0.7 \qquad = f^{-}_{\text{IV,I}}(g_{2,n})\,.
\end{aligned}
$$

This example illustrates two interesting properties. First, due to the need for compatible domains and ranges between stages, type I and type II structures cannot both appear in the same multiplier-saving cascade, even if separated by other types. Second, the technique described here never leads to more than four distinct gain values.

4.3. Leapfrog cascade

In cases where adjacent allpass stages with identical gains also lead to adjacent branch points or sums, pairs of multiplies from adjacent stages can be combined to lower the total multiplier count, sometimes all the way down to $N + 3$ for a cascade of N stages.

An example of this and the cascade type of multiplier reduction (§4.1) is shown in Figs. 5–6. Fig. 5 shows a cascade of four

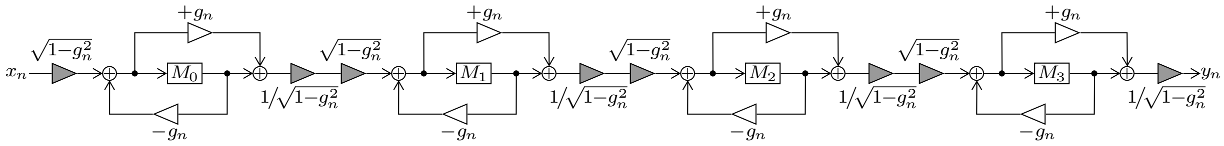

Figure 5: *Cascade of four 2-mult. (outside) allpass filters with identical time-varying gains g_n and different delays M_i, $i \in \{0 \cdots 3\}$.*

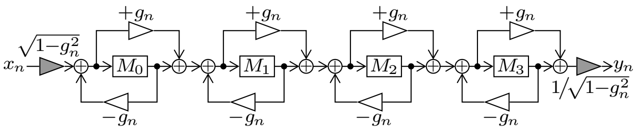

(a) *Eliminating reciprocal $1/\xi_{i,n}$ and $\xi_{i+1,n}$, $i \in \{0 \cdots 2\}$.*

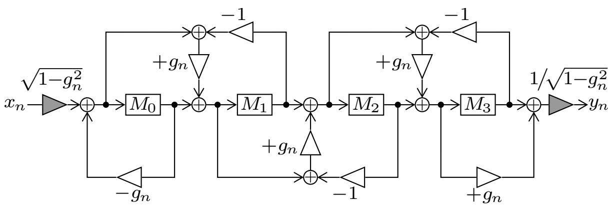

(b) *Combining $+g_{i,n}$ and $-g_{i+1,n}$, $i \in \{0 \cdots 2\}$.*

Figure 6: *Simplifying a cascade of several Schroeder allpasses.*

energy-preserving 2-mult. Schroeder allpasses. Fig. 6a shows the result of eliminating reciprocal multiplies. Fig. 6b shows the result of combining multiplies from adjacent stages. Note that in Fig. 6b, the even-numbered stages have been flipped vertically to keep the signal flow graph planar and easy to read. This structure resembles the classic "Leapfrog" filter topology from active filter synthesis [46]. Interestingly, besides the presence of the multiplies accomplishing the energy normalization, this and the same idea applied to 2-mult.$^\top$ yield identical structures to the "delay-sharing" allpass cascades proposed by Mitra and Hirano [44].

4.4. Nested allpass filters

In nesting structures [9–13] with identical allpass gains, we can also eliminate multiplications. To expose transformer multipliers to their inverses, we must *alternate* between "inside" and "outside" structures as we nest. In a realizable nested structure, the delay line is replaced with the cascade of one or more Schroeder allpasses and at least a one-sample delay. This means that one of the two pairs of reciprocal multipliers are not actually adjacent, only giving us the chance to save 1 multiplier per nesting, not 2.

4.5. Periodic gain modulation

A somewhat restrictive way to save multiplies is to only modulate the gains by certain *periodic* functions. When g_n is periodic in M, i.e., $g_n = g_{n-M}$, $\forall n$, the two transformer multiplies cancel out and hence can be eliminated, saving two multiplies. This can be seen by considering the "inside" proposed structures (Fig. 4). An equivalent filter is obtained by "pushing" ξ_n to the right through the length-M delay line, giving a composite multiplier ξ_{n-M}/ξ_n, which equals 1 (cancels out) when g_n is periodic in M.

5. CASE STUDY

Fig. 7a shows one proposed filter and delay M_{fb} inside a feedback loop. Feeding the system a single impulse, we expect the energy stored in the structure (1.0) to stay constant over time. The simulations are performed in GNU Octave, which uses double precision floating point numbers, using a sampling rate of $f_{\text{s}} = 44{,}100$ Hz, delay line lengths of $M_{\text{ap}} = 11$ and $M_{\text{fb}} = 101$, and gain g_n drawn randomly from uniform distribution $\mathcal{U}(-0.999, +0.999)$ over the 10 second simulation. The plotted value e_n is the deviation of the signal energy in the two delay lines from 1.0

$$e_n = 1.0 - \sqrt{\sum_{m=1}^{M_{\text{ap}}} u^2_{\text{ap},n-m} + \sum_{m=1}^{M_{\text{fb}}} u^2_{\text{fb},n-m}}\,, \tag{13}$$

where $u_{\text{ap},n-m}$ and $u_{\text{fb},n-m}$ are the mth samples in the delay lines.

Fig. 7b shows the energy error e_n for each of the structures. The absolute error is shown on the left-side axis; it is very small, on the order of 10^{-15}. In fact, the quantization to machine precision is visible. The spacing between representable numbers is called machine epsilon, $\varepsilon(e)$. For $e \in [1.0, 2.0[$, $\varepsilon(e) \approx 2.2204 \times 10^{-16}$; for $e \in [0.5, 1.0[$, $\varepsilon(e) \approx 1.1102 \times 10^{-16}$. The error, normalized to $\varepsilon(e)$, is shown on the right-side axis. This shows that the energy is preserved to machine precision, only picking up tens of εs over a 10 second (4.41×10^5 samples) simulation under strenuous coefficient variation. Each structure's average, minimum, and maximum for the simulation are given in Tab. 5.

6. CONCLUSIONS

We presented a family of 17 high-order Schroeder-style allpass filters which are canonic in delays and require (independent of filter order) a low number of adds (2 or 3), multiplies (3–6), and sign flips (0 or 1). No matter how the gain g_n parameterizing these filters is varied over time, these filters retain their energy preservation property. They also provide many alternatives for LTI implementations of the classic Schroeder filter. We also presented strategies for cascading and nesting them to reduce the total number of multiplies. These should be useful in various artificial reverb, digital audio effect, and sound synthesis applications which employ Schroeder allpass filters or 1st-order allpass filters.

7. ACKNOWLEDGMENTS

Thanks to François Germain, Andy Sarroff, and the anonymous reviewers for helpful feedback and to Ólafur Bogason for helpful discussions. Thanks to Ross Dunkel for helpful discussions on time-varying reactances, and also my apologies for failing to acknowledge them in [47].

Table 4: *Setting the gain $g_{i+1,n}$ of the $(i+1)$th stage to ensure that reciprocal multiplies can be eliminated, in terms of the previous (ith) stage's gain $g_{i,n}$. (Multi)function domains and ranges are shown as $\{domain\} \longrightarrow \{range\}$ if different from $]-1,+1[$.*

filter structure for the ith stage	filter structure for the $(i+1)$th stage: type I	type II	type III	type IV
type I	$f_{\text{I,I}} = \pm g_{i,n}$	$f_{\text{I,II}} = 0$ $\{0\} \longrightarrow \{0\}$	$f_{\text{I,III}} = +g_{i,n}^2/(2-g_{i,n}^2)$ $]-1,+1[\longrightarrow [0,+1[$	$f_{\text{I,IV}} = -g_{i,n}^2/(2-g_{i,n}^2)$ $]-1,+1[\longrightarrow]-1,0]$
type II	$f_{\text{II,I}} = 0$ $\{0\} \longrightarrow \{0\}$	$f_{\text{II,II}} = \pm g_{i,n}$	$f_{\text{II,III}} = -g_{i,n}^2/(2-g_{i,n}^2)$ $]-1,+1[\longrightarrow]-1,0]$	$f_{\text{II,IV}} = +g_{i,n}^2/(2-g_{i,n}^2)$ $]-1,+1[\longrightarrow [0,+1[$
type III	$f^{\pm}_{\text{III,I}} = \pm\sqrt{2g_{i,n}/(g_{i,n}+1)}$ $[0,+1[\longrightarrow]-1,+1[$	$f^{\pm}_{\text{III,II}} = \pm\sqrt{2g_{i,n}/(g_{i,n}-1)}$ $]-1,0] \longrightarrow]-1,+1[$	$f_{\text{III,III}} = +g_{i,n}$	$f_{\text{III,IV}} = -g_{i,n}$
type IV	$f^{\pm}_{\text{IV,I}} = \pm\sqrt{2g_{i,n}/(g_{i,n}-1)}$ $]-1,0] \longrightarrow]-1,+1[$	$f^{\pm}_{\text{IV,II}} = \pm\sqrt{2g_{i,n}/(g_{i,n}+1)}$ $[0,+1[\longrightarrow]-1,+1[$	$f_{\text{IV,III}} = -g_{i,n}$	$f_{\text{IV,IV}} = +g_{i,n}$

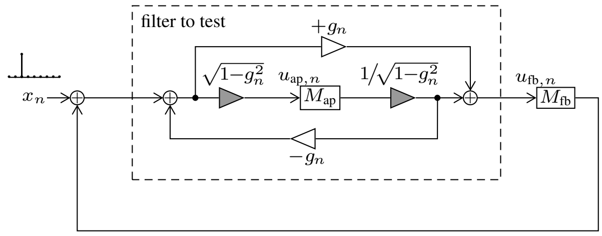

(a) *Block diagram of test setup.*

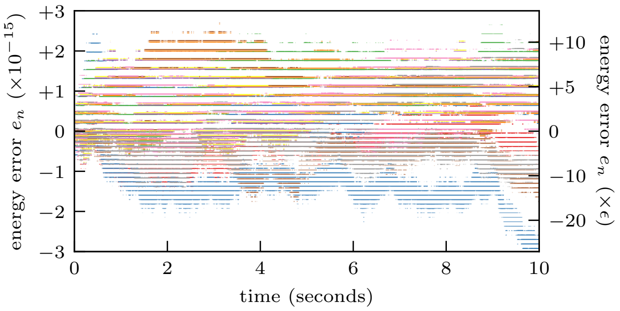

(b) *Error (absolute, and in # of machine εs) for all 17 structures.*

Figure 7: *Test of time-varying allpass filter in feedback loop. In the block diagram, the 2-mult. "inside" case is shown as an example.*

Table 5: *Error summary of 10 second test. Averages, minimums, and maximums (each $\times 10^{-16}$) for all 17 structures.*

Name	Avg.	Min	Max	Name	Avg.	Min	Max
1-mult., in.	−3.3	−15.5	−8.9	1-mult., out.	13.6	−32.2	4.4
1-mult.$^\top$, in.	8.4	−4.4	24.4	1-mult.$^\top$, out.	13.8	−2.2	26.6
2-mult., in.	9.8	−5.6	22.2	2-mult., out.	6.3	−7.8	22.2
2-mult.$^\top$, in.	10.0	−2.2	22.2	2-mult.$^\top$, out.	11.2	−4.44	26.7
3-mult., in.	9.8	−5.6	22.2	3-mult., out.	6.3	−7.8	22.2
3-mult.$^\top$, in.	10.0	−2.2	22.2	3-mult.$^\top$, out.	11.2	−4.4	26.7
4-mult., in.	−5.7	−17.8	4.4	4-mult., out.	10.1	−7.8	22.2
4-mult.$^\top$, in.	1.5	−7.8	13.3	4-mult.$^\top$, out.	2.2	−16.7	22.2
Normalized	−4.9	−14.4	8.9				

8. REFERENCES

[1] M. R. Schroeder and B. F. Logan, "'Colorless' artificial reverberation," *IRE Trans. Audio*, vol. 9, no. 6, pp. 209–214, Nov./Dec. 1961.

[2] M. R. Schroeder, "Natural sounding artificial reverberation," *J. Audio Eng. Soc.*, vol. 10, no. 3, pp. 219–223, July 1962.

[3] R. Väänänen, V. Välimäki, J. Huopaniemi, and M. Karjalainen, "Efficient and parametric reverberator for room acoustics modeling," in *Proc. Int. Comput. Music Conf.*, Thessaloniki, Greece, Sept. 1997.

[4] R. Väänänen, "Efficient modeling and simulation of room reverberation," MSc. thesis, Helsinki Univ. Technology, Finland, June 1997.

[5] L. Dahl and J.-M. Jot, "A reverberator based on absorbant all-pass filters," in *Proc. COST G-6 Conf. Digital Audio Effects*, Verona, Italy, Dec. 2000.

[6] S. J. Schlecht and E. A. P. Habets, "Time-varying feedback matrices in feedback delay networks and their application in artificial reverberation," *J. Acoust. Soc. Am.*, vol. 138, no. 3, pp. 1389–1398, Sept. 2015.

[7] M. A. Gerzon, "Unitary (energy-preserving) multichannel networks with feedback," *Electron. Lett.*, vol. 12, no. 11, pp. 278–279, May 1976.

[8] J. O. Smith III, *Physical audio signal processing for virtual musical instruments and audio effects*, W3K Pub., 2010.

[9] W. G. Gardner, *Applications of digital signal processing to audio and acoustics*, ch. Reverberation algorithms, pp. 85–131, Kluwer, New York, 2002, Ed. M. Kahrs and K. Brandenburg.

[10] V. Kot, "Digital sound effects echo and reverb based on non-exponentially decaying comb filter," in *Proc. 14th Europ. Signal Process. Conf.*, Florence, Italy, Sept. 2006.

[11] H. H. Lee, T. H. Kim, and J. S. Park, "Design of a digital artificial reverberation system using a dual all-pass filter," *J. Audio Eng. Soc.*, vol. 57, no. 3, pp. 121–130, Mar. 2009.

[12] M. R. Bai and H. Chen, "Comparative study of optimal design strategies of reverberators," *Open Acoust. J.*, vol. 2, pp. 31–44, 2009.

[13] J. h. Ahn and R. Dudas, "Musical applications of nested comb filters for inharmonic resonator effects," in *Proc. Int. Comput. Music Conf.*, Perth, Australia, Aug. 2013, pp. 226–231.

[14] S. J. Schlecht, "Frequency-dependent Schroeder allpass filters," *Appl. Sci.*, vol. 10, no. 1, 2020, Article #187.

[15] S. Bilbao, "Time-varying generalizations of allpass filters," *IEEE Signal Process. Lett.*, vol. 12, no. 5, pp. 376–379, May 2005.

[16] J. Pakarinen, M. Karjalainen, V. Välimäki, and S. Bilbao, "Energy behavior in time-varying fractional delay filters for physical modeling synthesis of musical instruments," in *Proc. Int. Conf. Acoust. Speech Signal Process.*, Philadelphia, PA, Mar. 2005, pp. 1–4.

[17] J. Pekonen, "Coefficient-modulated first-order allpass filter as distortion effect," in *Proc 11th Int. Conf. Digital Audio Effects*, Espoo, Finland, Sept. 2008, pp. 83–87.

[18] V. Välimäki, J. S. Abel, and J. O. Smith, "Spectral delay filters," *J. Audio Eng. Soc.*, vol. 57, no. 7/8, pp. 521–531, July/Aug. 2009.

[19] J. Pekonen, V. Välimäki, J. S. Abel, and J. O. Smith, "Spectral delay filters with feedback and time-varying coefficients," in *Proc. 12th Int. Conf. Digital Audio Effects*, Como, Italy, Sept. 2009, pp. 157–164.

[20] J. Kleimola, J. Pekonen, H. Penttinen, V. Välimäki, and J. S. Abel, "Sound synthesis using an allpass filter chain with audio-rate coefficient modulation," in *Proc. 12th Int. Conf. Digital Audio Effects*, Como, Italy, Sept. 2009, pp. 305–312.

[21] J. Kleimola, *Nonlinear abstract sound synthesis algorithms*, Ph.D. diss., Aalto Univ., Helsinki, Finland, 2013.

[22] J. Timoney, J. Pekonen, V. Lazzarini, and V. Välimäki, "Dynamic signal phase distortion using coefficient-modulated allpass filters," *J. Audio Eng. Soc.*, vol. 52, no. 9, pp. 596–610, Sept. 2014.

[23] G. Surges, T. Smyth, and M. Puckette, "Generative audio systems using power-preserving all-pass filters," *Comput. Music J.*, vol. 40, no. 1, pp. 54–69, Spring 2016.

[24] J. O. Smith, "A new approach to digital reverberation using closed waveguide networks," in *Proc. Int. Comput. Music Conf.*, Burnaby, Canada, Aug. 1985, pp. 47–53.

[25] T. Lokki and J. Hiipakka, "A time-variant reverberation algorithm for reverberation enhancement systems," in *Proc. COST G-6 Conf. Digital Audio Effects*, Limerick, Ireland, Dec. 2001.

[26] T. Choi, Y. C. Park, and D.-H. Youn, "Design of time-varying reverberators for low memory applications," *IEICE Trans. Inf. Systm.*, vol. E91-D, no. 2, pp. 379–382, Feb. 2008.

[27] S. J. Schlecht and E. A. P. Habets, "Reverberation enhancement systems with time-varying mixing matrices," in *Proc. 59th Int. Conf. Audio Eng. Soc.*, Montreal, Canada, July 2015.

[28] A. Fettweis, "Wave digital filters: Theory and practice," *Proc. IEEE*, vol. 74, no. 2, pp. 270–327, Feb. 1986.

[29] K. J. Werner, *Virtual analog modeling of audio circuitry using wave digital filters*, Ph.D diss., CCRMA, Stanford Univ., CA, Dec. 2016.

[30] J. D. Markel and A. H. Gray Jr., *Linear prediction of speech*, Springer-Verlag, Berlin, Germany, 1976.

[31] A. H. Gray Jr. and J. D. Markel, "Digital lattice and ladder filter synthesis," *IEEE Trans. Audio Electroacoust.*, vol. 21, no. 6, pp. 491–500, Dec. 1973.

[32] A. H. Gray Jr. and J. D. Markel, "A normalized digital filter structure," *IEEE Trans. Acoust., Speech, Signal Process*, vol. 23, no. 3, pp. 268–277, June 1975.

[33] J. L. Kelly and C. C. Lochbaum, "Speech synthesis," in *Proc. 4th Int. Cong. Acoust.*, Copenhagen, Denmark, Sept. 1962, pp. 1–4.

[34] T. S. Stilson, *Efficiently-variable non-oversampled algorithms in virtual-analog music synthesis—a root-locus perspective*, Ph.D. diss., CCRMA, Stanford Univ., CA, June 2006.

[35] P. R. Cook and G. P. Scavone, "PRCRev class reference," online, 1995, `https://ccrma.stanford.edu/software/stk/classstk_1_1PRCRev.html`.

[36] B. Schottstaedt, "CLM," online, unknown, `https://ccrma.stanford.edu/software/snd/snd/clm.html`.

[37] K. Barr, "Audio effects: Reverberation," online, unknown, `http://www.spinsemi.com/knowledge_base/effects.html#Reverberation`.

[38] S. Costello, "RIP Keith Barr," online, Aug. 2010, `https://valhalladsp.wordpress.com/2010/08/25/rip-keith-barr/`.

[39] J. Dattorro, "Effect design, part 1: Reverberator and other filters," *J. Audio Eng. Soc.*, vol. 45, no. 9, pp. 660–684, Sept. 1997.

[40] J. M. Chowning, J. M. Grey, J. A. Moorer, and L. Rush, "Computer simulation of music instrument tones in reverberant environments," STAN-M 1, CCRMA, Stanford Univ., CA, June 1974.

[41] J. A. Moorer, "Signal processing aspects of computer music: A survey," *Proc. IEEE*, vol. 65, no. 8, pp. 1108–1137, Aug. 1977.

[42] P. R. Samson, "A general-purpose digital synthesizer," *J. Audio Eng. Soc.*, vol. 26, no. 3, pp. 106–113, Mar. 1980.

[43] J. A. Moorer, "About this reverberation business," *Comput. Music J.*, vol. 3, no. 2, pp. 13–28, June 1979.

[44] S. K. Mitra and K. Hirano, "Digital all-pass networks," *IEEE Trans. Circuits Systems*, vol. 21, no. 5, pp. 688–700, Sept. 1974.

[45] D. C. Massie, "An engineering study of the four-multiply normalized ladder filter," *J. Audio Eng. Soc.*, vol. 41, no. 7/8, pp. 564–582, July/Aug. 1993.

[46] F. E. J. Girling and E. F. Good, "The leapfrog or active-ladder synthesis," *Wireless World*, vol. 76, no. 1417, pp. 341–345, July 1970.

[47] Ó. Bogason and K. J. Werner, "Modeling time-varying reactances using wave digital filters," in *Proc. 21st Int. Conf. Digital Audio Effects*, Aveiro, Portugal, Sept. 2018, pp. 272–279.

A. PROOF OF COMMUTABILITY OF $\mathbf{\Lambda}$ AND $\mathbf{\Xi}$

Two-port *scattering* matrices $\mathbf{S}$ and *transfer scattering* matrices $\mathbf{T}$ relate a pair of incident waves a_1 and a_2 to a pair of reflected waves b_1 and b_2 at ports 1 and 2 according to

$$\begin{bmatrix} b_1 \\ b_2 \end{bmatrix} = \begin{bmatrix} s_{11} & s_{12} \\ s_{21} & s_{22} \end{bmatrix} \begin{bmatrix} a_1 \\ a_2 \end{bmatrix} \quad , \quad \begin{bmatrix} b_1 \\ a_1 \end{bmatrix} = \begin{bmatrix} t_{11} & t_{12} \\ t_{21} & t_{22} \end{bmatrix} \begin{bmatrix} a_2 \\ b_2 \end{bmatrix} .$$

Here, the time index n is suppressed for compactness. These matrices can be related to one another in the following way

$$\mathbf{S} = \frac{1}{t_{22}} \begin{bmatrix} t_{12} & \Delta_{\mathbf{T}} \\ 1 & -t_{21} \end{bmatrix} \quad , \quad \mathbf{T} = \frac{1}{s_{21}} \begin{bmatrix} -\Delta_{\mathbf{S}} & s_{11} \\ -s_{22} & 1 \end{bmatrix} , \tag{14}$$

where $\Delta_{\mathbf{T}}$ and $\Delta_{\mathbf{S}}$ are the determinants of $\mathbf{T}$ resp. $\mathbf{S}$:

$$\Delta_{\mathbf{T}} = t_{11}t_{22} - t_{12}t_{21} \quad , \quad \Delta_{\mathbf{S}} = s_{11}s_{22} - s_{12}s_{21} .$$

In the transfer formalism, cascades are described by matrix multiplication, i.e., a cascade of K stages with transfer matrices $\mathbf{T}_k$, $k \in \{1 \cdots K\}$ is simply $\prod_{k=1}^{K} \mathbf{T}_k$.

Now consider our transformer characterized by parameter ξ with scattering matrix

$$\mathbf{\Xi} = \begin{bmatrix} 0 & 1/\xi \\ \xi & 0 \end{bmatrix} \quad \text{i.e.} \quad \begin{matrix} \xi_{11} = 0 & \xi_{12} = 1/\xi \\ \xi_{21} = \xi & \xi_{22} = 0 \end{matrix} .$$

By (14), its transfer scattering matrix $\mathbf{T}_{\mathbf{\Xi}}$ is

$$\mathbf{T}_{\mathbf{\Xi}} = \begin{bmatrix} 1/\xi & 0 \\ 0 & 1/\xi \end{bmatrix} = \mathbf{I}/\xi \quad \text{i.e.} \quad \begin{matrix} t_{\xi,11} = 1/\xi & t_{\xi,12} = 0 \\ t_{\xi,21} = 0 & t_{\xi,22} = 1/\xi \end{matrix} ,$$

where $\mathbf{I}$ is the 2×2 identity matrix.

The scaled identity matrix $\mathbf{I}/\xi$ commutes with any other matrix, meaning that for any transfer scattering matrix $\mathbf{T}_{\mathbf{\Lambda}}$,

$$\mathbf{T}_{\Pi} = \underbrace{\mathbf{T}_{\mathbf{\Lambda}}(\mathbf{I}/\xi)}_{\mathbf{T}_{\mathbf{\Lambda\Xi}}} = \underbrace{(\mathbf{I}/\xi)\mathbf{T}_{\mathbf{\Lambda}}}_{\mathbf{T}_{\mathbf{\Xi\Lambda}}} \quad , \quad \begin{matrix} t_{\Pi,11} = \dfrac{t_{\lambda,11}}{\xi} & t_{\Pi,12} = \dfrac{t_{\lambda,12}}{\xi} \\ t_{\Pi,21} = \dfrac{t_{\lambda,21}}{\xi} & t_{\Pi,22} = \dfrac{t_{\lambda,22}}{\xi} \end{matrix} .$$

This shows that $\mathbf{T}_{\mathbf{\Lambda\Xi}}$, the transfer scattering relationship of $\mathbf{\Lambda}$ cascaded with $\mathbf{\Xi}$, is identical to $\mathbf{T}_{\mathbf{\Xi\Lambda}}$, the transfer scattering relationship of $\mathbf{\Xi}$ cascaded with $\mathbf{\Lambda}$. We will call them interchangeably $\mathbf{T}_{\mathbf{\Pi}}$. Hence, they have the same scattering matrix $\mathbf{\Pi}$ given by

$$\mathbf{\Pi} = \begin{bmatrix} \lambda_{11} & \lambda_{12}/\xi \\ \lambda_{21}\xi & \lambda_{22} \end{bmatrix} \quad \text{i.e.} \quad \begin{matrix} \pi_{11} = \lambda_{11} & \pi_{12} = \lambda_{12}/\xi \\ \pi_{21} = \lambda_{21}\xi & \pi_{22} = \lambda_{22} \end{matrix} .$$